Original Article

Enhancement of Digital Mammography Images Using Neutrosophic Divergence Score Based on Intuitionistic Fuzzy Entropy

Leila Pourreza[1], Nasser Aghazadeh[1,2,3], Mahdi Hashemzadeh[4]

[1]Department of Mathematics, Azarbaijan Shahid Madani University, Tabriz, Iran, [2]Department of Mathematics, Izmir Institute of Technology, Izmir, Türkiye, [3]Center for Theoretical Physics, Khazar University, 41 Mehseti Street, Baku, AZ1096, Azerbaijan, [4]Faculty of Information Technology and Computer Engineering, Azarbaijan Shahid Madani University, Tabriz, Iran

Abstract

Background: Uncertainty in medical images—especially mammograms—caused by low contrast and insufficient brightness creates difficulties in detecting masses and microcalcifications. These limitations often lead to diagnostic uncertainty for radiologists, making effective image enhancement essential for accurate clinical assessment. **Aims and Objectives:** This study aims to develop an improved method for digital mammography image enhancement that reduces uncertainty, improves contrast, and preserves fine details to support more accurate diagnosis. **Materials and Methods:** The proposed method integrates intuitionistic fuzzy entropy and neutrosophic sets (NSs) in a five-stage framework: (1) Transforming the input image into an intuitionistic fuzzy set; (2) Applying intuitionistic fuzzy entropy to reduce ambiguity; (3) Converting the image to an NS representation; (4) Enhancing image details using the neutrosophic divergence score (NDS); (5) Improving contrast through fuzzy histogram hyperbolization. Performance was evaluated on two benchmark mammography datasets using quantitative metrics, including the contrast improvement index, discrete entropy, absolute mean brightness coefficient, absolute mean brightness error, and the naturalness image quality evaluator, as well as a qualitative visual assessment. **Results:** Experimental results show that the proposed method surpasses existing approaches, including intuitionistic fuzzy sets, type-2 fuzzy sets, and neutrosophic-based enhancement methods. It achieves superior contrast enhancement, preserves naturalness, and effectively highlights fine mammographic details. **Conclusion:** The method substantially reduces uncertainty in mammography images, enhancing diagnostic visibility and supporting improved accuracy for radiologists. Its strong performance across fatty, fatty-glandular, and dense-glandular breast tissues makes it a promising component for future computer-aided diagnosis systems.

Keywords: *Fuzzy divergence score, histogram hyperbolization, image enhancement, intuitionistic fuzzy entropy, intuitionistic fuzzy set, mammography, neutrosophic divergence score, neutrosophic set, type-2 fuzzy set*

Submitted: 26-May-2025 **Revised:** 31-Aug-2025 **Accepted:** 15-Sep-2025 **Published:** 30-Mar-2026

Introduction

Breast cancer is the most frequently diagnosed malignancy among women worldwide and remains the leading cause of cancer-related mortality, thereby representing a major global health challenge.[1] It usually starts in the milk glands (lobules) of the breast or the ducts that carry milk from the breast to the nipple, and rarely starts in the breast fat or fibrous tissue.[2] Signs of breast cancer include a lump in the breast, change in breast shape or change in the color of the breast tissue. Digital mammography is the most effective method of early detection of this disease, as it allows early detection of lumps or abnormal lesions.[3] However, interpretation of mammogram images is difficult for radiologists because of variability in grey matter levels in breast tissue, which may result in incorrect diagnosis. Computer-aided diagnosis systems assist radiologists in achieving higher diagnostic accuracy by enhancing the contrast of mammographic images without affecting their brightness. By improving image contrast while maintaining consistent brightness levels, these systems provide clearer visualization of breast tissue structures, thereby supporting radiologists in making more accurate and reliable diagnostic decisions.[4]

Several methods have been proposed for enhancing the quality of digital mammography, most of which are based on histogram equalization.[5] In this method,

Address for correspondence:
Prof. Nasser Aghazadeh, Department of Mathematics, Azarbaijan Shahid Madani University, Tabriz, Iran.
E-mail: aghazadeh@azaruniv.ac.ir, nasseraghazadeh@iyte.edu.tr

Access this article online

Website: www.jmssjournal.net

DOI: 10.4103/jmss.jmss_50_25

Quick Response Code:

How to cite this article: Pourreza L, Aghazadeh N, Hashemzadeh M. Enhancement of digital mammography images using neutrosophic divergence score based on intuitionistic fuzzy entropy. J Med Signals Sens 2026;16:9.

the contrast increase of the image depends on the histogram expansion, and the values of the output pixels of the image are calculated by the cumulative distribution function of the histogram of the input image. However, histogram equalization sometimes has undesirable effects, such as excessive contrast intensification, abnormal discontinuity in soft areas of the image, and noise sensitivity. The method of contras limited adaptive histogram equalization (CLAHE) is used to overcome these problems. In this method, the increase of contrast around the pixels is dependent on the slope of the cumulative distribution function of the grey level of the pixels in the same region. Before calculating the cumulative function, the histogram is scaled to a predefined size, and the pixels that are removed are uniformly added to the other pixels in the histogram. Then, a histogram equalization is applied to each area of the image.[6] However, the manual determination of the histogram cropping value makes this method less suitable for the enhancement of mammogram images. Another method, called un-sharp masking, is also used to enhance the images obtained by mammography. This method works in a similar way to high-pass filters and well highlights image details such as edges, but it is highly susceptible to noise.[7]

The above methods cannot adequately address the problems of noise and low contrast in mammography images. Fuzzy approaches help improve the visual quality of images by exploiting uncertainties, particularly membership functions. Among them, contrast enhancement is one of the most widely used operators, where modifying the membership function improves the image contrast.[8] Another method is fuzzy histogram hyperbolization, which uses a logarithmic function to correct the gray levels of the image according to the nonlinear perception of brightness by humans. However, these methods are sometimes not suitable for enhancing mammography images due to excessive contrast enhancement. To overcome this problem, there are other fuzzy methods using the IF-THEN fuzzy rule.[6] One of these methods is the fuzzy contrast-limited adaptive histogram equalization (FC-CLAHE). In this method, the image is first transferred to the fuzzy domain. Then, on the basis of an algorithm that matches the pixel intensities with fuzzy rules, the histogram threshold value is determined for each region of the image.

Finally, histogram equalization is performed for each region. Unlike contrast limited adaptive histogram equalization, this method does not require a manually selected threshold; however, it is still less effective in enhancing fine details in mammography images. Since mammography images are typically low-contrast and contain blurred details, more advanced fuzzy approaches, such as type-2 fuzzy sets and intuitionistic fuzzy sets, have been suggested in.[4] These methods have caught the attention of medical imaging researchers.[9-13] Various intuitive fuzzy enhancement methods proposed in a number of research[14-16] and type-2 fuzzy set have also been used for improving image quality.[14,17] In type-2 fuzzy set methods, the membership function is defined ambiguously and fuzzily and lies in a range between high and low membership levels. However, intuitive fuzzy methods usually perform better than type-2 fuzzy sets in improving the image quality of mammography, as they preserve the information, shape, and brightness of the image without increasing noise. Although advanced fuzzy techniques are more effective in increasing the contrast of mammogram images compared to non-fuzzy and traditional fuzzy techniques, sometimes the fine detail in the image is not fully enhanced by the increase in contrast.

In 1980, Smarandache introduced the concept of neutrosophic sets (NSs) within the philosophical framework of neutrosophy.[3] Neutrosophic theory assigns to every element three degrees of membership, reflecting its truth, indeterminacy, and falsity values. These sets have found widespread application in image processing tasks that leverage indeterminate information, owing to their ability to effectively handle such uncertainties. NSs have been successfully employed in image enhancement and noise reduction. A noise reduction method using NSs, incorporating entropy and a γ-median filter to mitigate uncertainty and noise, was proposed in.[18] Similarly, in the study by Bharti and Mittal,[19] an ultrasound image is enhanced by converting the image to a neutrosophic domain and applying a neutrosophic similarity score to enhance the image quality. The neutrosophic similarity score was also used to enhance the pathological image described in.[20] This score, which measures the similarity of two elements in the NS, was introduced in 2014 by Guo *et al*.[21] A method to enhance a limited set of mammogram images by using a neutrosophic difference score is presented in.[3] In this approach, the mammogram is first transformed to the neutrosophic domain. Subsequently, the image quality is enhanced by a neutrosophic divergence score (NDS) and then a fuzzy histogram hyperbolization to increase contrast. This method demonstrates strong performance in highlighting fine details in mammographic images.

The proposed method uses an intuitive fuzzy entropy function to reduce ambiguity in the mammogram. Specifically, by combining the intuitionistic fuzzy entropy concept with the NDS from the study by Chaira,[3] the method aims to enhance contrast while preserving detail in various types of digital mammography images, including fatty, dense glandular, and fatty-glandular mammography.

The structure of the paper is as follows: Section 2 presents preliminaries and related work, Section 3 describes the proposed method, Section 4 reports the experimental results, and Section 5 provides the conclusion and directions for future work.

Preliminaries and Related Work

Intuitionistic fuzzy set

Fuzzy set theory, originally proposed by Zadeh,[22] was developed to mathematically model and represent

uncertainty within sets. This uncertainty is expressed by the membership function. While fuzzy methods provide a useful framework for uncertainty modeling, they may become inadequate in scenarios involving increased uncertainty. To address this shortcoming, Atanassov formulated the theory of intuitionistic fuzzy sets in 1985.[23] In the Atanassov method proposed, two types of uncertainty are considered: membership function and non-membership function. In fuzzy sets, the non-membership function is defined as the complement of the membership function. However, in intuitive fuzzy sets (IFS), the nonmembership function can be less than or equal to the complement of the membership function. This difference of "less than" is created due to the uncertainty in the definition of the membership function. For a finite set $X = \{x_1, x_2, \ldots x_n\}$, an IFS is represented as:

$$A_{IFS} = \left\{\left(x, \mu_A(x), \nu_A(x)\right) | x \in X\right\} \quad (1)$$

Where $\mu(x)$ and $\upsilon_A(x)$ represent the membership and non-membership functions, respectively, satisfying:

$$0 \le \mu_A(x) + \nu_A(x) \le 1 \quad (2)$$

The membership function $\mu(x)$ can take different shapes, including Gaussian, gamma, triangular, or other common forms. Meanwhile, the non-membership function $\upsilon_A(x)$ is generated using an intuitionistic fuzzy generator, such as those proposed by Sugeno, Yager, or similar models. The condition in equation (2), $\mu_A(x) + \upsilon_A(x) \le 1$, accounts for the hesitation that arises during the definition of the membership function. The hesitation function, denoted by $\pi_A(x)$, satisfies, $\pi_A(x) \le 1$. Consequently, considering all three functions, the following relationship is obtained

$$\mu_A(x) + \nu_A(x) + \pi_A(x) = 1 \quad (3)$$

An intuitionistic fuzzy generator operates similarly to a fuzzy negation or complement, but with a key difference in its formal definition. Specifically, a function qualifies as an intuitionistic fuzzy generator if it satisfies the condition $\upsilon_A(x) \le 1 - \mu_A(x)$. The inequality here ($\upsilon_A(x)$ being strictly $<1 - \mu_A(x)$ in some cases) captures the hesitation inherent in assigning membership degrees. When there's no hesitation present, the intuitionistic fuzzy set simplifies to a conventional fuzzy set, i.e., $\upsilon_A(x) = 1 - \mu_A(x)$.

Intuitionistic fuzzy entropy

Ambiguity, as a feature of incomplete information, occurs when there is no clear separation between elements that belong to a set and those that do not, meaning that the set boundaries are uncertain. To address such uncertainty, entropy was first introduced by Zadeh[22] in 1965 and has since been widely used in research. The term "entropy" was selected because its equations resemble those of Shannon's entropy, although they measure different types of uncertainty. In fuzzy theory, entropy is obtained from a geometric interpretation of intuitionistic fuzzy sets and is based on the distances between them.[8] The term entropy was chosen because of the inherent similarity between its equations and Shannon entropy, although these two measures fundamentally quantify different types of uncertainty. In this context, entropy is derived from a geometric interpretation of fuzzy sets and is based on relations between them, which are related by distances. In 1972, De Luca and Termini introduced certain requirements that reflect our intuitive understanding of the degree of ambiguity.[24] In 1975, Kaufmann proposed that the degree of ambiguity of a fuzzy set A be measured by the metric distance between its membership function and the membership function (or characteristic function) of its nearest crisp set. Furthermore, in 1979, Yager defined the degree of ambiguity in terms of the lack of distinction between a fuzzy set and its complement.[8]

Neutrosophic set

NS for a finite set $X = \{x_1, x_2, \ldots, x_n\}$ is defined as Equation (4):

$$A_{NS} = \left\{\left(x, T_A(x), I_A(x), F_A(x)\right) | x \in X\right\} \quad (4)$$

Where $T_A : X \to [0,1], I_A : X \to [0,1]$ and $F_A : X \to [0,1]$

denote the truth, indeterminacy, and falsity membership functions, respectively. There is no restriction on the sum of $T(x)$, $I_A(x)$ and $F_A(x)$.

$$0 \le Sup\, T_A(x) + Sup\, I_A(x) + Sup\, F_A(x) \le 3 \quad (5)$$

Neutrosophic divergence measure

To distinguish between two entities, whether in theoretical or practical contexts, specific criteria are always required. This principle also applies to intuitionistic fuzzy sets. In the following, two measures – distance and similarity – for intuitionistic fuzzy sets are introduced.

Distance measure

The function $D : IFS \times IFS \to [0, +\infty]$ is a distance measure

between two elements of an intuitionistic fuzzy set if the following properties hold for any two intuitionistic fuzzy sets, such as A_{IFS} and B_{IFS}.

1. $D(A_{IFS}, B_{IFS}) = D(B_{IFS}, A_{IFS})$

2. For any three arbitrary intuitionistic fuzzy sets A_{IFS}, B_{IFS} and C_{IFS} Where $A_{IFS} \subseteq B_{IFS} \subseteq C_{IFS}$ the following relationships hold:

$D(A_{IFS}, B_{IFS}) \le D(A_{IFS}, C_{IFS})$ and

$D(B_{IFS}, C_{IFS}) \le D(A_{IFS}, C_{IFS})$.

3. $A_{IFS} = B_{IFS} \Leftrightarrow D(A_{IFS}, B_{IFS}) = 0$

4. For any arbitrary intuitionistic fuzzy sets A_{IFS}, $B_{IFS}, 0 \le D(A_{IFS}, B_{IFS}) \le 1$.

Similarity measure

The function $S: IFS \times IFS \to [0,+\infty]$ is a similarity measure between two elements of an intuitionistic fuzzy set if the following properties hold for any two intuitionistic fuzzy sets, such as A_{IFS} and B_{IFS}:

1) $\mathrm{S}(A_{IFS}, B_{IFS}) = S(B_{IFS}, A_{IFS})$

2. For any three arbitrary intuitionistic fuzzy sets A_{IFS}, B_{IFS} and C_{IFS} Where $A_{IFS} \subseteq B_{IFS} \subseteq C_{IFS}$ the following relationships hold: $S(A_{IFS}, B_{IFS}) \geq S(A_{IFS}, C_{IFS})$ and $(B_{IFS}, C_{IFS}) \geq S(A_{IFS}, C_{IFS})$.

3) $A_{IFS} = B_{IFS} \Leftrightarrow S(A_{IFS}, B_{IFS}) = 1$

4) For any arbitrary intuitionistic fuzzy sets A_{IFS}, $B_{IFS}, 0 \leq S(A_{IFS}, B_{IFS}) \leq 1$.

Suppose f is a monotonically decreasing function. Since $0 \leq D(A_{IFS}, B_{IFS}) \leq 1$, it follows that: $f(1) \leq f(D(A_{IFS}, B_{IFS})) \leq f(0)$, thus the normalized similarity measure can be expressed as:

$$0 \leq \frac{f(D(A_{IFS}, B_{IFS})) - f(1)}{f(0) - f(1)} \leq 1.$$

Therefore, the similarity measure between two arbitrary intuitionistic fuzzy sets, such as A_{IFS} and B_{IFS}, is defined as:

$$\mathrm{S}(A_{IFS}, B_{IFS}) = \frac{f(D(A_{IFS}, B_{IFS})) - f(1)}{f(0) - f(1)}$$

Assuming $f(x) = 1 - x$, the similarity measure is given by:

$S(A_{IFS}, B_{IFS}) = 1 - D(A_{IFS}, B_{IFS})$, since $f(1) = 0$ and $f(0) = 1$.

A distance measure, termed the intuitionistic fuzzy divergence, was introduced in.[25] This measure utilizes three parameters: The membership function, the non-membership function, and the hesitation function.

Suppose $A_{IFS} = \{(x, \mu_A(x), \nu_A(x)) | x \in X\}$ and $B_{IFS} = \{(x, \mu_B(x), \nu_B(x)) | x \in X\}$ are two intuitionistic fuzzy sets. Considering the hesitation function, the membership function range for the intuitionistic fuzzy sets A and B is given by $[\mu_A(x), \mu_A(x) + \pi_A(x)]$ and $[\mu_B(x), \mu_B(x) + \pi_B(x)]$. The distance is determined based on the hesitation or lack of knowledge in assigning values to the membership function.

Now, assume A and B are two images, with a_{ij} and b_{ij} representing the pixel values at position (i, j) in images A and B, respectively. The intuitionistic fuzzy divergence between the pixels of images A and B is defined as follows:

$$\begin{aligned} IFD(A,B) = \sum_i \sum_j \Big(& 2 - \left[1 - \mu_A(a_{ij}) + \mu_B(b_{ij})\right] e^{\mu_A(a_{ij}) - \mu_B(b_{ij})} \\ & - \left[1 - \mu_B(b_{ij}) + \mu_A(a_{ij})\right] e^{\mu_B(b_{ij}) - \mu_A(a_{ij})} + 2 \\ & - \left[1 - \mu_A(a_{ij}) - \mu_B(b_{ij}) + \pi_B(b_{ij}) \right. \\ & \left. - \pi_A(a_{ij})\right] e^{\mu_A(a_{ij}) - \mu_B(b_{ij}) - (\pi_B(b_{ij}) - \pi_A(a_{ij}))} \\ & - \left[1 - (\pi_B(b_{ij}) - \pi_A(a_{ij})) \right. \\ & \left. + (\mu_A(a_{ij}) - \mu_B(b_{ij}))\right] e^{\pi_B(b_{ij}) - \pi_A(a_{ij}) - (\mu_A(a_{ij}) - \mu_B(b_{ij}))} \Big) \end{aligned}$$

The new neutrosophic divergence measure is calculated using fuzzy divergence.[26] In this method, the image itself, denoted as P, is compared in the neutrosophic domain with respect to an ideal image in terms of divergence. Suppose the ideal image in the neutrosophic domain is represented as B For an ideal image, the truth membership value is 1, the indeterminacy membership value is 0, and the falsity membership value is also 0.

Fuzzy histogram hyperbolization

Fuzzy histogram hyperbolization was introduced by Tizhoosh and Fochem.[27] as a method for image enhancement. In this technique, a membership function is first defined to calculate pixel membership values. Then, a fuzzifier such as β, which acts as a linguistic hedge, is applied with a logarithmic transformation to adjust the membership function. For neutrosophic image enhancement, a modified version of fuzzy histogram hyperbolization, as described in the study by Chaira,[3] is used to improve image quality.

Proposed Method

The proposed method aims to exploit two key features: the intuitionistic fuzzy sets and the generalized form of these sets, known as NSs. Using an intuitionistic fuzzy entropy function, this method minimizes the uncertainty inherent in the image. Subsequently, by utilizing the capacity of NSs to handle indeterminate information, an enhanced image is generated, which visually improves even the subtle details of mammographic images. The steps of the image enhancement process are illustrated in Figure 1. The proposed method comprises five main stages: In the first stage, the input image is transformed into an intuitionistic fuzzy set. In the second stage, the intuitionistic fuzzy entropy function is applied to the image. In the third stage, the resulting image is converted into an NS. In the fourth stage, an NDS is applied to the image obtained from the previous stage. Finally, in the fifth stage, to enhance the image contrast, a fuzzy histogram hyperbolization technique based on a nonlinear logarithmic function is employed to produce the final enhanced image.

Figure 1: Stages of the proposed method

Application of intuitionistic fuzzy set

In this stage, the following steps are undertaken:

Step 1: An image within the fuzzy set framework is represented as an ordered triple comprising brightness intensity, a membership function, and a non-membership function. This is mathematically formulated as:

$$I_{IFS} = \left\{\left(a, \mu_A(a), \nu_A(a)\right) | a \in \{0,1,2,\ldots,L-1\}\right\} \tag{6}$$

In this context, the input image is a grayscale image with L = 256 levels.

Step 2: The input image is transferred to the fuzzy domain through normalization

$$\mu_i\left(a_{xy}\right) = \frac{a_{xy} - a_{min}}{a_{max} - a_{min}} \tag{7}$$

Here, a_{xy} represents the grayscale value of the pixel located at position (x, y) in the image. a_{min} and a_{max} denote the minimum and maximum values of the input image, respectively. The intuitionistic membership function, as described in,[23] is expressed as follows:

$$\mu_{IFS}\left(a_{xy};k\right) = 1 - \left(1 - \mu_{IFS}\left(a_{xy};k\right)\right)^{k-1} \tag{8}$$

Step 3: The non-membership function is defined based on the fuzzy generator function

$$\vartheta_{IFS}\left(a_{xy};k\right) = \left(1 - \mu_{IFS}\left(a_{xy};k\right)\right)^{k(k-1)} \tag{9}$$

Step 4: Given that the sum of the membership and non-membership functions in an intuitionistic fuzzy set is less than or equal to 1, the hesitation function is expressed as follows:

$$\pi_{IFS}\left(a_{xy};k\right) = 1 - \mu_{IFS}\left(a_{xy};k\right) - \vartheta_{IFS}\left(a_{xy};k\right) \tag{10}$$

Application of intuitionistic fuzzy entropy

Mammogram images are often characterized by uncertainties in pixel intensity, which affect the decision-making of radiologists when analyzing digital mammograms. IFS is an effective approach to reducing this ambiguity. In this method, not only the membership function but also the non-membership function is used to resolve the uncertainty. Given the difficulties in the precise selection of these membership functions, the inclusion of a hesitation function is essential. Intuitive fuzzy entropy is used to optimize and fine-tune these functions. The steps in this process are described as follows:

Step 1: To obtain the optimal value of k, the intuitionistic fuzzy entropy function introduced in the study by Vlachos and Sergiadis[28] is used, which is calculated as follows:

$$E\left(I_{IFS};k\right) = \frac{1}{MN}\sum_{x=0}^{M-1}\sum_{y=0}^{N-1}\frac{2\mu_{IFS}\left(a_{xy};k\right)\vartheta_{IFS}\left(a_{xy};k\right) + \pi_{IFS}{}^{2}\left(a_{xy};k\right)}{\pi_{IFS}{}^{2}\left(a_{xy};k\right) + \mu_{IFS}{}^{2}\left(a_{xy};k\right) + \vartheta_{IFS}{}^{2}\left(a_{xy};k\right)} \tag{11}$$

Step 2: The optimal value of k is the one that maximizes the relationship given in equation (11).

Therefore, the suitable value of k is calculated as follows:

$$k_{optm} = \max\left(E\left(I_{IFS};k\right)\right) \tag{12}$$

Step 3: The image is represented in the intuitionistic fuzzy domain by incorporating the optimal value k_{optm} as follows:

$$I_{IFSoptm} = \{(a_{xy}, \mu_{IFS}\left(a_{xy};k_{optm}\right), \nu_{IFS}\left(a_{xy};k_{optm}\right) | a_{xy} \in \{0,1,2,\ldots,L-1\} \tag{13}$$

Step 4: The Atanassov operator D_β, as described in the study by Vlachos and Sergiadis,[29] is applied after refining the intuitionistic fuzzy components to transform the image from the intuitionistic fuzzy domain back to the fuzzy domain, as follows:

$$D_\beta(I_{IFSoptm}) = \{a_{xy}, \mu_{IFS}\left(a_{xy}\right) + \beta\pi_{IFS}\left(a_{xy}\right), \vartheta_{IFS}\left(a_{xy}\right) + (1-\beta)\pi_{IFS}\left(a_{xy}\right) | \beta \in [0,1]\} \tag{14}$$

Step 5: In the fuzzy domain, different images are obtained by varying the value of β. The optimal value of β is determined using the ambiguity index described in,[26] calculated as follows:

$$\beta_{optm} = \begin{cases} 0 & \beta_{optm} < 0 \\ \beta_{optm} & 0 \le \beta_{optm} \le 1 \\ 1 & \beta_{optm} > 1 \end{cases} \tag{15}$$

Where

$$\beta_{optm} = \frac{\sum_{g=0}^{L-1} h_I(g)\pi_{IFS}\left(g;k_{optm}\right)\left(1 - 2\mu_{IFS}\left(g;k_{optm}\right)\right)}{2\sum_{g=0}^{L-1} h_I(g)\pi_{IFS}{}^{2}\left(g;k_{optm}\right)} \tag{16}$$

Where g represents the grayscale intensity value, h_I denotes the histogram value of the image.

Step 6: The image in the fuzzy domain is transformed into the spatial domain using the following conversion, and the

defuzzified image is calculated as follows:

$$a_{xy}^{'} = (L-1)\,\mu_{D_\beta}\left(I_{IFSoptm}\left(a_{xy}\right)\right) \tag{17}$$

Where

$$\mu_{\beta_D}\left(I_{IFSoptem}\left(a_{xy}\right)\right) = \beta_{optm} + \left(1-\beta_{optm}\right)\mu_{IFS}\left(a_{xy};k_{optm}\right) - \beta_{optem}\vartheta_{IFS}\left(a_{xy}:k_{optm}\right) \tag{18}$$

At this stage, the final image is obtained after applying the intuitionistic fuzzy entropy function, resulting in an image with reduced ambiguity compared to the initial image.

Application of neutrosophic set

In this stage, the obtained image is transformed into an NS to utilize the indeterminate information of the image for the enhancement process. To achieve this, the following steps are performed:

Step 1: The image $a_{xy}^{'}$ is normalized as follows:

$$mem(A) = \frac{a_{xy}^{'}(i,j) - \min\left(a_{xy}^{'}\right)}{\max\left(a_{xy}^{'}\right) - \min\left(a_{xy}^{'}\right)} \tag{19}$$

Step 2: The processed image undergoes segmentation into non-overlapping 5 × 5 pixel windows. For each local window region, we first compute the standard deviation of pixel intensities. Subsequently, the membership degree for each pixel within a given window is derived by offsetting its intensity value with the window's standard deviation *std(window)*.[30] The membership function for each window is calculated as follows:

$$mem_{window} = mem(A) - std(window) \tag{20}$$

mem_{window} represents the membership value of the pixels within a window. This is calculated for all windows, and ultimately, the membership matrix *me*(*A*) is computed.

Step 3: The truth membership function is calculated as follows:

$$mem(A) = \frac{a_{xy}^{'}(i,j) - \min\left(a_{xy}^{'}\right)}{\max\left(a_{xy}^{'}\right) - \min\left(a_{xy}^{'}\right)} \tag{21}$$

The indeterminacy membership function is calculated separately using the gradient and Shannon entropy. Initially, the gradient for each pixel is computed using the Prewitt operator as follows:

$$I_{A_G} = \frac{Gd(i,j) - Gd_{min}}{Gd_{max} - Gd_{min}} \tag{22}$$

Where $G(i,j)$ is the gradient value of the grayscale image at coordinates (i,j), Gd_{max} and Gd_{min} are the maximum and minimum gradient values of the image, respectively.

The Shannon entropy is calculated for each 5 × 5 window. The entropy value at pixel coordinates (i,j) as introduced in the study by Chaira,[30] is computed as follows:

$$E_w(i,j) = -\left[p_w \log\left(p_w\right) + \left(1-p_w\right)\log\left(1-p_w\right)\right] \tag{23}$$

Where p_w represents a 5 × 5 pixel neighborhood around the pixel at position (i,j) in the image. For each window, the entropy matrix is calculated, and ultimately, the overall entropy matrix is obtained.

Step 4: Assuming $I_{A_E} = \frac{E_A}{\max\left(E_A\right)}$ is the entropy matrix and using equations (22) and (23), the indeterminacy value I_A is computed by combining them with the fuzzy t-norm. The fuzzy t-norm is a binary operator that allows the evaluation of the intersection of two fuzzy subsets. Various types of fuzzy t-norms exist. In this method, the Łukasiewicz t-norm is used, defined as follows:

$$I_A = \max\left(I_{A_E} + I_{A_G} - 1, 0\right) \tag{24}$$

Step 5: The falsity membership function is calculated using the following relationship:

$$F_A = 1 - T_A \tag{25}$$

A pixel of image A at coordinates $(i,)$, denoted as $A(i,j)$, in the NS framework is defined as follows:

$$P(i,j) = \left\{T_A(i,j), I_A(i,j), F_A(i,j)\right\} \tag{26}$$

Where $T(i,j)$, $I_A(i,j)$ and $F_A(i,j)$ respectively, represent the membership functions for bright pixels, indeterminate pixels, and non-bright pixels of the image.

Application of neutrosophic divergence score

The NDS is employed to determine the divergence between two arbitrary images within an NS framework. The divergence score between a pixel (i,j) in the neutrosophic domain and the ideal image in the same domain is calculated as follows:

$$\begin{aligned} Div_{score}(P(i,j),B) = \\ \sum_{j=1}^{N}\sum_{i=1}^{N}\Big(2-\left(1-T_A(i,j)+T_B(i,j)\right)e^{(T_A(i,j)-T_B(i,j))} - \\ \left(1-T_B(i,j)+T_A(i,j)\right)e^{(T_B(i,j)-T_A(i,j))} + \\ 2-\left(1-I_A(i,j)+I_B(i,j)\right)e^{(I_A(i,j)-I_B(i,j))} - \\ \left(1-I_B(i,j)+I_A(i,j)\right)e^{(I_B(i,j)-I_A(i,j))} + \\ 2-\left(1-F_A(i,j)+F_B(i,j)\right)e^{(F_A(i,j)-F_B(i,j))} - \\ \left(1-F_B(i,j)+F_A(i,j)\right)e^{(F_B(i,j)-F_A(i,j))}\Big). \end{aligned} \tag{27}$$

Since image B represents an ideal neutrosophic image, it is assumed that $T(i,j) = 1$, $I_B(i,j) = 0$ and $F_B(i,j) = 0$. Consequently, the divergence score between the image A

and the ideal image B, as expressed in Equation (27), can be formulated as follows:

$$Div_{score}(P(i,j),B) = \sum_{j=1}^{N}\sum_{i=1}^{N}\Big(2-\big(2-T_A(i,j)\big)e^{(T_A(i,j)-1)} - \big(T_A(i,j)\big)e^{(1-T_A(i,j))} + 2-\big(1-I_A(i,j)\big)e^{(I_A(i,j))} - \big(1+I_A(i,j)\big)e^{(-I_A(i,j))} + 2-\big(1-F_A(i,j)\big)e^{(F_A(i,j))} - \big(1+F_A(i,j)\big)e^{(-F_A(i,j))}\Big) \quad (28)$$

Subsequently, the image most like the ideal image is determined using the Neutrosophic Divergence Score, calculated as follows:

$$NDS(i,j) = 1 - Div_{Score(P(i,j)B)} \Big/ \max\left(Div_{Score}\right) \quad (29)$$

Application of fuzzy histogram hyperbolization

The foundation of fuzzy histogram hyperbolization was established by Tizhoosh and Fochem.[27] The technique begins with the selection of an appropriate membership function to determine membership values for image pixels. A fuzzifier parameter β – functioning as a linguistic hedge – is then applied to adjust the membership function through logarithmic transformation. Building upon this framework, our proposed method for neutrosophic image enhancement incorporates an advanced version of fuzzy histogram hyperbolization, as detailed in the study by Chaira.[3]

$$\mu_{enh} = \log\left(\mu_{new}^{\beta} + 1\right) \quad (30)$$

where

$$\beta = -\alpha\mu_{new} + 2 \quad (31)$$

and

$$\alpha = mean\left(\mu_{new}\right) \quad (32)$$

The new image obtained from Equation (30) represents the final enhanced image.

Experiments and Results

Evaluating the performance of contrast enhancement algorithms in medical imaging, particularly in low-contrast mammography, is a challenging task. To achieve reliable conclusions, both qualitative and quantitative assessments are typically performed in parallel. This section first introduces the datasets employed in the experiments, followed by a description of the evaluation criteria used to assess the performance of the proposed method and to compare it with existing approaches. Finally, the experimental results are presented and discussed in terms of both qualitative (visual) and quantitative evaluations, highlighting the effectiveness of the proposed contrast enhancement method.

Dataset

In this study, experiments were conducted using images from the MIAS data set[31] and a subset of images from the CBIS-DDSM dataset.[32]

MIAS dataset

The MIAS dataset consists of 322 digital mammogram images, in which breast tissue is categorized into three types: Fatty, fatty-glandular, and dense-glandular. Based on the severity and type of abnormality, the images are further classified into several categories, including well-defined (circumscribed) masses, architectural distortions, bilateral asymmetry, microcalcifications, spiculated masses, ill-defined masses, and normal cases. Each abnormality is also labeled as either benign or malignant. The dataset provides ground truth annotations determined by expert radiologists, including the coordinates of the lesion center, the radius of the lesion, and the lesion type. All images are publicly available, with a resolution of 1024 × 1024 pixels.

CBIS-DDSM dataset

The Curated Breast Imaging Subset of the Digital Database for Screening Mammography (CBIS-DDSM) dataset, a curated subset of the Digital Database for Screening Mammography (DDSM), consists of 3,103 digitized mammographic images. These images were carefully selected and validated by expert radiologists. The collection includes both benign and malignant cases, each supported by confirmed pathological diagnoses. In addition, the dataset provides ground-truth annotations, including segmentation masks of regions of interest and detailed abnormality descriptions. The images are grouped into two main categories: masses (891 cases) and calcifications (753 cases). The dataset is further divided into a training set of 2458 images (79.2%) and a testing set of 645 images (20.8%).

In this study, the algorithms for various contrast enhancement methods were implemented in the MATLAB 2018 environment.

Evaluation metrics

A wide range of metrics has been developed to assess the quality of natural images; however, only a limited number of measures are specifically available for evaluating medical image quality, as it is strongly linked to interpretability and diagnostic accuracy. As a result, relying solely on quantitative metrics may not fully reflect the visual quality of medical images, since each metric focuses on a particular aspect of image characteristics. To address this limitation, the performance of the proposed method is evaluated from both qualitative (visual) and quantitative perspectives. In this study, the quantitative image quality metrics employed to assess the proposed method include the contrast improvement index (CII), discrete entropy (DE), absolute mean brightness coefficient (AMBC), absolute mean brightness error (AMBE), and the natural

image quality evaluator (NIQE). The definitions of these metrics are presented below:

Discrete entropy function

This function is used to quantify the information content in an image after enhancement. It represents the randomness or uncertainty within the image. The DE for measuring uncertainty in the enhanced image is defined as follows:

$$Entropy\left(E\right)=\sum_{x,y=0}^{N-1}\left(-P_{xy}lnP_{xy}\right) \tag{33}$$

The term P_{xy} denotes the probability of the intensity value of a pixel at coordinates (x, y) in the image. In other words, DE serves as a metric to quantify the variability in the distribution of pixel intensities within the image.

Absolute mean brightness error

This is defined as the absolute difference between the mean of the input image I_{xy} and the resulting image $\tilde{I}_{xy}$, expressed as follows

$$AMBE=\left| I_{xy}-\tilde{I}_{xy}\right| \tag{34}$$

Absolute mean brightness coefficient

After calculating the mean values of the input image *A* and the output image B, denoted as *M*(A) and *M*(*B*), respectively, the normalized absolute mean brightness coefficient $AMBC_N \in [0,1]$ is defined as follows.

$$AMBC_N=\frac{1}{1+\left|M\left(A\right)-M\left(B\right)\right|} \tag{35}$$

The closer the value of $AMBC_N$ is to one, the better the brightness of the image is preserved, and vice versa.

Image contrast represents the degree of difference between the dark and bright regions of an image. When the difference between the maximum brightness intensity and the minimum brightness intensity is small, the mammography image will exhibit low contrast.

Contrast improvement index

This is an evaluation metric for assessing the improvement in the contrast of an image, defined as follows:

$$CII=\frac{C_{output}}{C_{input}} \tag{36}$$

C_{output} and C_{input} represent the mean total contrast values in the output image and the inputimage, respectively. The contrast is defined as follows:

$$C=\frac{f_m-b_m}{f_m+b_m} \tag{37}$$

Where *fm* represents the mean gray level of the foreground, and *bm* represents the mean gray level of the background. The higher the value of the CII, the better the quality of the output image.

Natural image quality evaluator

The image quality may be impaired by distortions such as noise, blur or other artifacts introduced during the capture and processing of the image. Considerable efforts were made to develop objective metrics for assessing the quality of the images. If a distortion-free reference image is not available, nonreference quality metrics such as the natural image quality evaluator may be used. No-reference algorithms use the statistical properties of the input image to evaluate the quality of the image. A lower NIQE indicates that the processed image is more natural and has a higher quality.

Experimental results and comparison with other methods

In this section, the performance of the proposed method is compared with conventional approaches, including methods based on type-2 fuzzy sets, intuitionistic fuzzy methods, and enhancement techniques utilizing NDSs, from both quantitative and qualitative (visual) perspectives. For quantitative evaluation of the performance of various enhancement methods, the evaluation metrics introduced in Evaluation metrics are employed. In addition, the qualitative (visual) performance of the proposed method, compared to other enhancement techniques, is presented using a selection of sample images from the MIAS database. To assess the generalizability of the proposed method and to further evaluate the performance of enhancement methods from both qualitative (visual) and quantitative perspectives, a number of images from the CBIS-DDSM database are also utilized.

Qualitative comparison of the proposed method with other methods

From the radiologist's point of view, the contrast enhancement in the mammogram image is assessed by visualizing the boundaries and margins of the mass. In this section, to assess the qualitative performance of the proposed method, it is compared with type-2 fuzzy methods, including Chaira[33] and BT,[34] the intuitive fuzzy method IFS,[11] and the NDS-based method NS.[3] For this assessment, three MIAS images and four CBIS-DDSM images were used. Three images from the set presented in section 4.1, namely the images mdb152, mdb 202, and mdb 179, are used in Figure 2. These images are shown in row (a) of Figure 2. The reference images are also shown in the row (g) of Figure 2. In addition, Figure 2 compares the performance results of the proposed method with the four other methods.

Figure 2, Column (A) first row (a) displays the image mdb152 from the MIAS dataset. This image depicts breast cancer with a fatty background tissue and a benign architectural distortion. For this image, the method Chaira[33] in (b), based on type-2 fuzzy sets, results in excessive contrast enhancement in several parts of the image, leading to overall image saturation. The third row

(c) in this column shows the effects of the BT enhancement method, based on type-2 fuzzy sets, as presented in the study by Bora and Thakur.[34] This method improves the visual quality of the digital mammogram to some extent but also exhibits regional saturation in areas with architectural distortion. The next row (d) shows the enhanced image using the IFS method.[11] This method provides a better visual quality than the Type-2 fuzzy method but does not optimally increase contrast. While the contrast and visual clarity of the lesions are enhanced, the noise intensification in the image obscures the details of the lesions, which makes them less disjointed in the final image. The next row (e) displays the enhanced image using the NS method proposed in the study by Chaira.[3] This method offers better visual quality than type-2 fuzzy-based methods and introduces less ambiguity compared to the IFS method, though it lacks adequate contrast while preserving image details. The final row (f) in this column presents the enhanced image using the proposed method. As observed, this method delivers superior visual quality compared to type-2 fuzzy-based methods, introduces less ambiguity than the IFS method, and effectively enhances contrast. In this image, the benign architectural distortion, appearing as a circular shape in the center, is clearly visible in the row (g) of Figure 2.

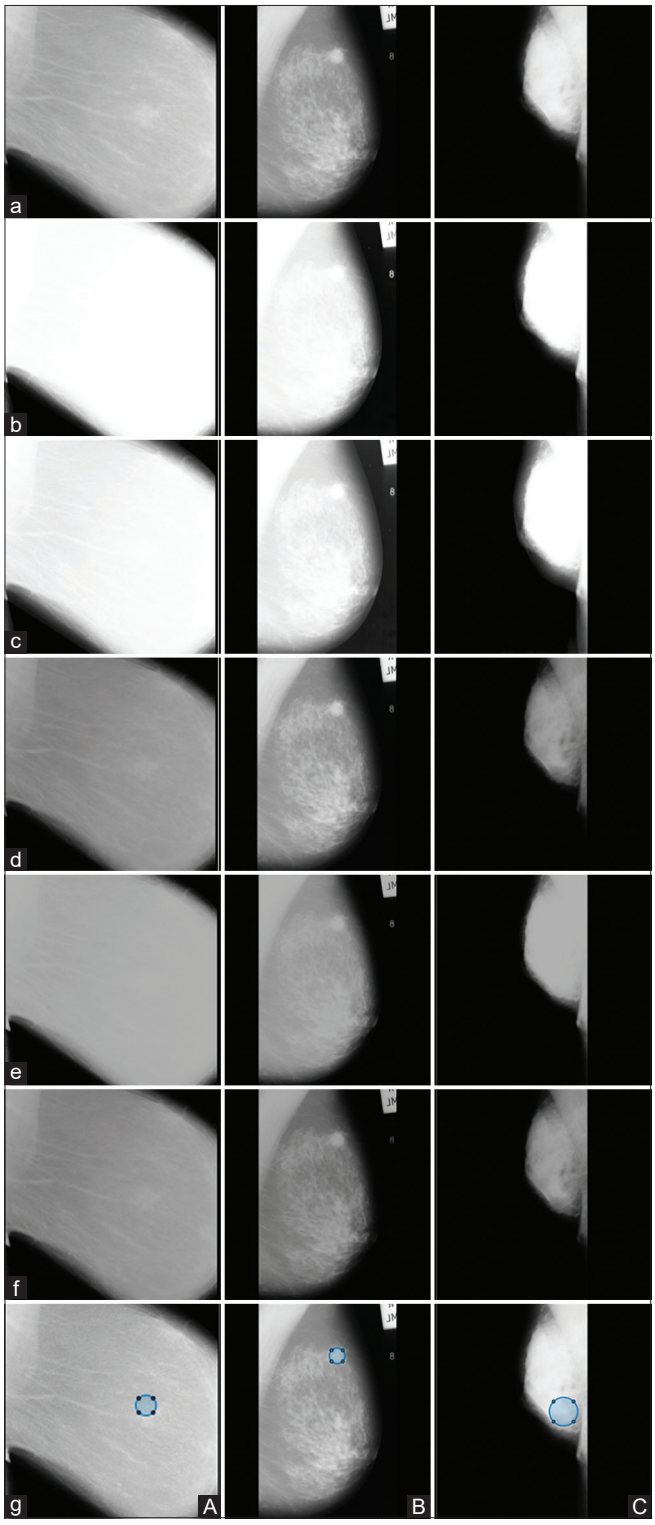

Figure 2: Visual comparison of the proposed method's results with other methods. (a) Three original images: mdb 152, mdb 202, and mdb179, (b) Results by Chaira,[33] (c) Results by BT,[34] (d) Results by intuitive fuzzy sets,[11] (e) Results by neutrosophic set,[3] (f) Results by proposed method, and (g) Ground truth

Challenges in mammography

One of the main challenges for radiologists is to detect masses in images of dense breast tissue. The dense breast tissue appears white, and breast masses are also white, while fatty tissue appears almost black. White masses are easier to detect on a black background, but white masses are difficult to detect on a white background. This can reduce the accuracy of detecting and classifying the type of mass in mammograms of breasts with dense glandular tissue. Improving these images could increase the accuracy of detecting and classifying the type of lesion.

Column (B) first row (a) displays the image mdb202 from the MIAS dataset, which represents a breast with dense tissue and a spiculated malignant mass. The second row (b) in this column shows the enhanced image using the Chaira method,[33] based on type-2 fuzzy sets. This method causes excessive contrast enhancement in several parts of the image, resulting in overall image saturation. The next row (c) presents the BT enhancement method, based on type-2 fuzzy sets.[34] This technique improves the visual quality of the digital mammogram to some extent but also shows regional saturation in areas containing the mass. The next row (d) displays the enhanced image using the IFS method.[11] This method provides better visual quality than type-2 fuzzy-based methods; however, it does not optimally enhance contrast. While contrast and visual clarity of lesions are improved, noise amplification in the image obscures lesion details, making them less discemible in the resulting image. The next row (e) shows the enhanced image using the NS method.[3] This method offers better visual quality than type-2 fuzzy-based methods, introduces less ambiguity than the IFS method, and, as observed, still

does not a contrast enhancement. The final row (e) presents the enhanced image using the proposed method, which delivers superior visual quality compared to type-2 fuzzy-based methods, introduces less ambiguity than the IFS method, and effectively enhances contrast.

Column (C) first row (a) displays the image mdb179 from the MIAS dataset, which shows breast cancer in dense glandular tissue with low contrast and a spiculated malignant mass. The second row (b) in this column shows the enhanced image using the Chaira method,[33] which results in excessive saturation in several regions of the image, with visible artifacts at the bottom edge. The following row (c) presents the results of the BT method,[34] which increases the density of the dense breast image, consequently obscuring abnormalities in whitened regions. The subsequent row (d) shows the enhanced image using the IFS method,[11] based on intuitionistic fuzzy sets, which may reduce ambiguity in mammography images. This method provides a better visual quality than type-2 fuzzy-based methods, but does not improve the overall visual quality of the image, since the details of the lesion are not highlighted, and the contour of the abnormality is not clearly visible. The next row (e) displays the enhanced image using the NS method,[3] based on NSs. As is evident, this method, despite low contrast, fails to highlight the spiculated malignant mass located in the lower-right corner. The final row (f) presents the result of the proposed method, which provides superior visual quality without loss of information, maintaining naturalness and brightness. In this image, the spiculated malignant mass in the lower-right corner is clearly visible in the row (g) of Figure 2.

To evaluate the performance of the proposed method, a number of images from the CBIS-DDSM database were also utilized. In Figure 3, four images – namely, Calc_Test_P_00202_RIGHT_CC, Calc_Training_P_00016_LEFT_CC, Mass_Test_P_00202_RIGHT_CC, and Mass_Test_P_00116_RIGHT_CC – are used. These images are displayed in the first row of Figure 3. The images in this database have varying dimensions; for instance, the image Calc_Test_P_00038_RIGHT_CC has dimensions of 4688 × 2744, while the image Calc_Training_P_00048_RIGHT_CC has dimensions of 5816 × 3920. In this study, to facilitate a more effective comparison of the performance of enhancement methods across different image types, implementations were performed on images resized to dimensions of 1024 × 1024. In addition, to highlight the location of masses and calcifications, reference images from the dataset were overlaid on the original images, and these are visible in the last row of Figure 3. In Figure 3, the qualitative (visual) performance results of the proposed method are compared with those of four other methods.

Figure 3, columns A and D, show the P_00202. This image shows breast cancer with a grade 1 breast density and contains two types of lesions: one is a malignant, clustered calcification visible in column A, and the other is a mass visible in column D. In Figure 3, row (b), the Chaira method[33] results in excessive contrast enhancement in several parts of the image. Row (c) shows the effects of the BT method, based on type-2 fuzzy sets as proposed in the study by Bora and Thakur,[34] which slightly improves the visual quality of the image. Row (d) shows the enhanced image based on the IFS method, using the intuitive fuzzy approach proposed in the study by Dabass *et al*.[11] This method provides better visual quality than the type-2 fuzzy-based methods; however, it does not optimize or enhance contrast. While contrast and visual clarity of the lesions are enhanced, the noise intensification in the image obscures the details of the lesions and renders them less visible in the resulting image. Row (e) shows an enhanced NS-based Image using the NS approach as proposed in the study by Chaira.[3] This method offers better visual quality than type-2 fuzzy-based methods and produces less ambiguity compared to the intuitive fuzzy method, though it lacks adequate contrast while preserving image details. The final row (f) in this column displays the enhanced image based on the proposed method. As observed, this method delivers superior visual quality compared to type-2 fuzzy-based methods, introduces less ambiguity than the intuitive fuzzy method, and effectively enhances contrast, making details clearly visible.

Column B shows Calc_Training_P_00016_LEFT_CC image containing the calcification lesion. Row (b) the Chaira method[33] also causes excessive contrast enhancement in several parts of the image. Row (c) demonstrates the effects of the BT method, based on type-2 fuzzy sets as proposed in the study by Bora and Thakur,[34] which similarly results in excessive contrast, thereby failing to improve the visual quality of the image. Row (d) in this column shows the enhanced image based on the IFS method, utilizing the intuitive fuzzy approach proposed in.[11] This method provides better visual quality compared to type-2 fuzzy-based methods; however, it does not optimally enhance contrast. While contrast and visual clarity of lesions are improved, noise amplification in the image obscures lesion details, making them less discemible in the resulting image. Row (e) shows the enhanced image based on the NS method, employing the NS approach proposed in the study by Chaira.[3] This method offers better visual quality than type-2 fuzzy-based methods and produces less ambiguity compared to the intuitive fuzzy method, though it lacks adequate contrast while preserving image details. The next row (f) in this column displays the enhanced image based on the proposed method. As observed, this method delivers superior visual quality compared to type-2 fuzzy-based methods, introduces less ambiguity than the intuitive fuzzy method, and effectively enhances contrast, making details clearly visible.

Column C displays the image Mass_Test_P_00116_RIGHT_CC. This image shows breast cancer with a grade

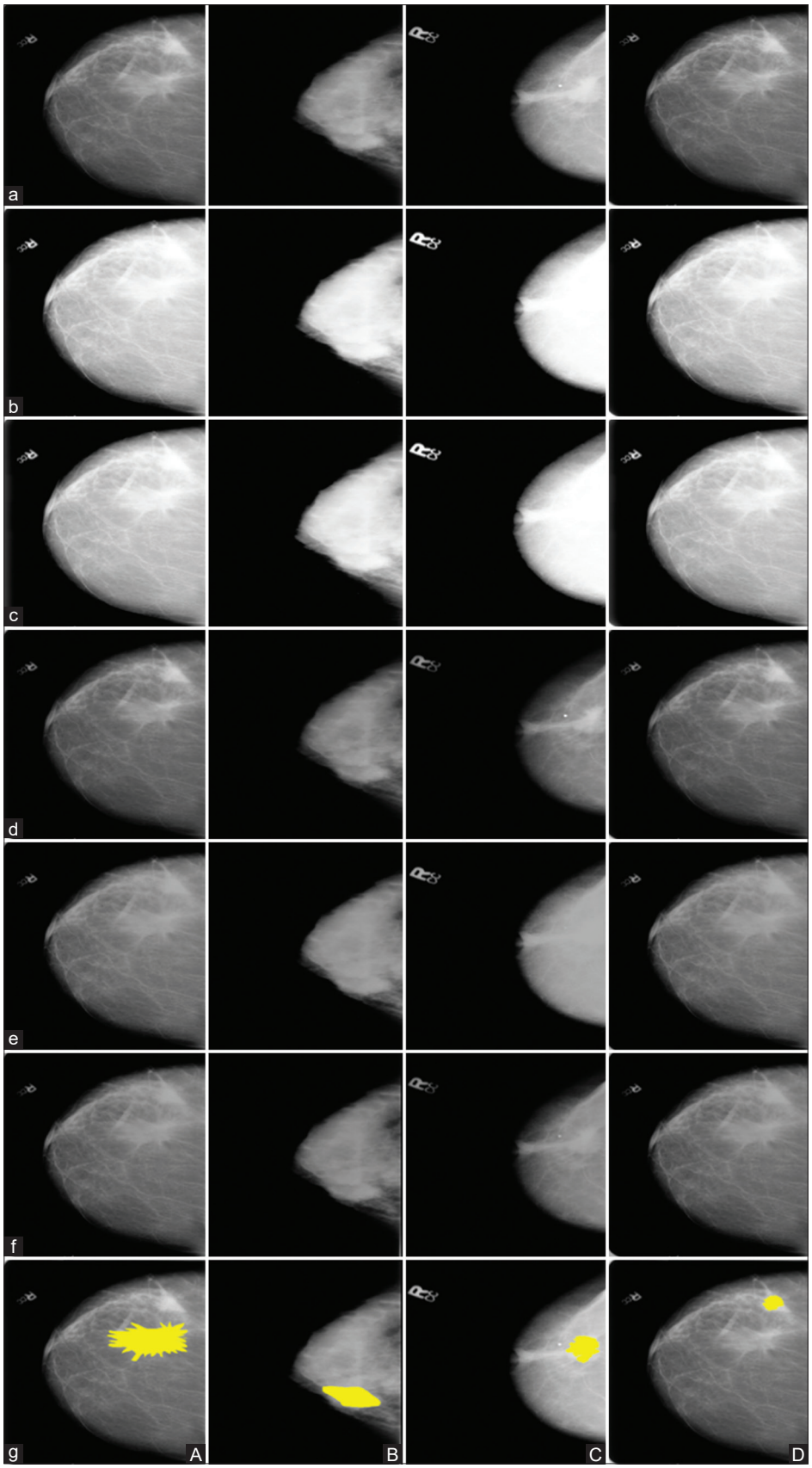

Figure 3: Visual comparison of the proposed method's results with other methods: (a) Four Original Image: Calc_Test_P_00202_RIGHT_CC, Calc_Training_P_00016_LEFT.CC, Mass_Test_P_00116_RIGHT.CC, and Mass_Test_P_00202_RIGHT.CC, (b) Result by Chaira,[33] (c) Result by BT,[34] (d) Result by IFS,[11] (e) Result by NS,[3] (f) Result by Proposed Method and (g) Ground truth overlied on original image

2 breast density and contains a malignant mass with an irregular shape. Row (b), the Chaira method[33] causes excessive contrast enhancement in several parts, leading to overall image saturation. Row (c) shows the effects of the BT method, based on type-2 fuzzy sets as proposed in,[34] which also results in overall image saturation. Row (d) in this column shows the enhanced image based on the IFS method, utilizing the intuitive fuzzy approach proposed in.[11] This method provides better visual quality compared to type-2 fuzzy-based methods; however, it does not optimally enhance contrast. While contrast and visual clarity of lesions are improved, noise amplification in the image obscures lesion details, making them less discemible in the resulting image. Row (e) shows the enhanced image based on the NS method, employing the NS approach proposed in.[3] This method offers better visual quality than type-2 fuzzy-based methods and produces less ambiguity compared to the intuitive fuzzy method, though it lacks adequate contrast while preserving image details. Row (f) in this column displays the enhanced image based on the proposed method. As observed, this method delivers superior visual quality compared to type-2 fuzzy-based methods, introduces less ambiguity than the intuitive fuzzy method, and effectively enhances contrast, making details clearly visible.

Quantitative comparison of the proposed method with other methods

Quantitative evaluation metrics play a critical role in comparing the overall performance of different image enhancement methods. In this section, we compare the results of various enhancement methods applied to the image dataset introduced in Evaluation metrics, based on quantitative evaluation metrics. The metrics used for this purpose include the CII, AMBE, AMBC, DE, and NIQE. The results of these experiments are presented graphically in Figures 4-8. In these figures, the values of the aforementioned evaluation metrics, obtained by different methods for each image in the dataset, are compared.

Figure 4 shows that enhanced digital mammograms based on the proposed method exhibit a high CII. Conversely, enhancement methods relying on type-2 fuzzy set demonstrate poor contrast, with lower CII values.

Figure 5 compares the AMBE values for different enhancement methods. The graph in Figure 5 shows that the proposed method has a relatively low AMBE value for most images, which demonstrates the effectiveness of the proposed method in correcting the contrast of digital mammography without affecting the brightness.

Figure 6 presents a comparative evaluation of AMBC values in relation to brightness preservation. It is evident that the proposed method delivers optimal AMBC values for the majority of images, underscoring its effectiveness in preserving the natural appearance of the original image.

Figure 7 shows a comparison of DE values, which indicate the degree of uncertainty and randomness of the improved images. As the graph in Figure 7 shows, the proposed method has less entropy than the intuitive fuzzy-based methods and the NS method, which is due to the fact that noise is eliminated, and details are highlighted only in the mass portion of the image.

As mentioned, the MIAS dataset does not have ground truth images to accurately identify masses and defects, so the NIQE criterion is used to examine the degree of naturalness of the images obtained from various improvement methods. In this paper, the MATLAB library command has been used to measure this criterion.

Figure 8 shows a comparison of NIQE values, which indicate the naturalness of the enhanced images. As the graph in Figure 8 shows, the proposed method provides relatively better image quality than other enhancement methods.

Finally, to review the overall quantitative results obtained, the average performance of the proposed method compared to the average of other improvement methods according to the evaluation criteria used in the trials is summarized in Table 1. A comparison of the column relating to the CII assessment criterion shows that the proposed method,

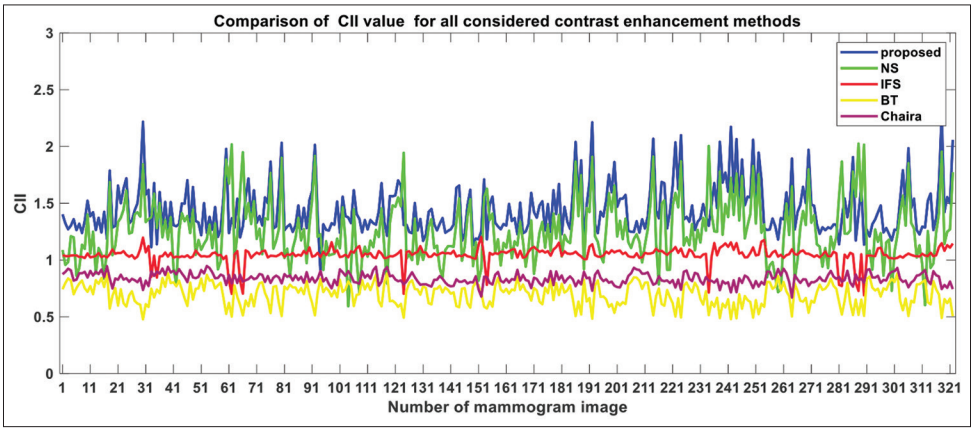

Figure 4: Comparative analysis of contrast improvement index values for the applied enhancement methods. CII – Contrast improvement index

with a value of 1.4452, has the highest increase in the CII, whereas the BT method, with a value of 0.6991, is the lowest of all methods. In the column relating to the AMBC assessment criterion, the NS method is the most successful in preserving the natural brightness of the image, with a value of 0.9885. In this comparison, the proposed method, with an average of 0.9517, has an acceptable value in maintaining the natural brightness of the images after the IFS method. In this criterion, the Chaira method, with an average of 0.6543, has the lowest value, which shows that this method is weak in maintaining the natural brightness of the images compared to other methods. In the column related to the AMBE evaluation criterion, the NS method with a mean value of 0.0117 shows the lowest value in correcting the contrast of digital mammography without affecting the brightness. In this comparison, the proposed method, with a mean of 0.0513, has an acceptable value in correcting the contrast of digital mammography without affecting the brightness after the IFS method. In this criterion, the BT method with a mean value of 0.1467 has the highest value, which shows that this method is weak in correcting the contrast of digital mammography without affecting the brightness compared to other methods. In the column related to the DE evaluation criterion, the IFS method, with a mean of 0.0232, shows the highest level of uncertainty and randomness compared to other methods. In this criterion, the proposed method, with a mean of 2.6718, has the highest level of uncertainty and randomness after the NS method, with a mean of 2.6821. In this criterion, the BT method, with a mean of 2.2544, shows the lowest level of uncertainty and randomness compared to other methods. In the column related to the NIQE evaluation criterion,

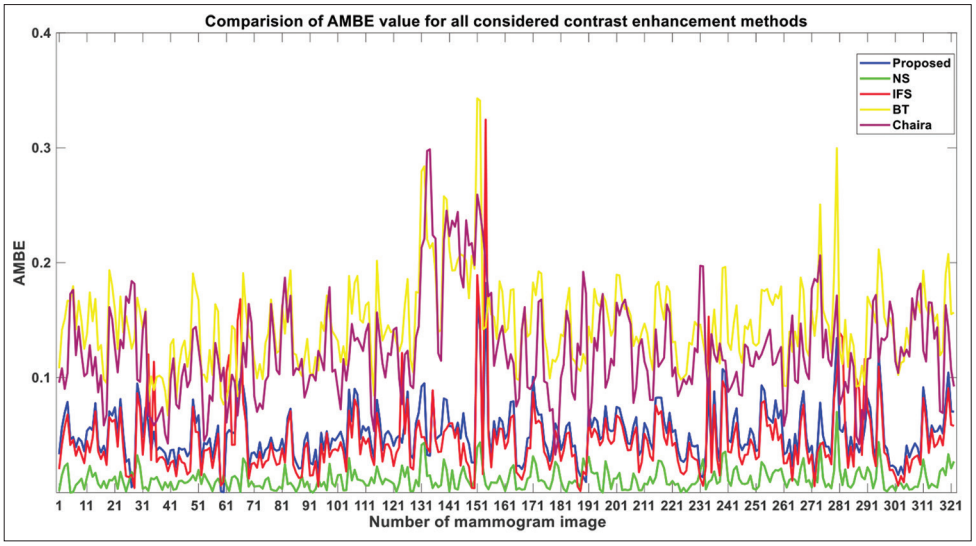

Figure 5: Comparative analysis of absolute mean brightness error values for the applied enhancement methods with lower contrast improvement index values. AMBE – Absolute mean brightness error

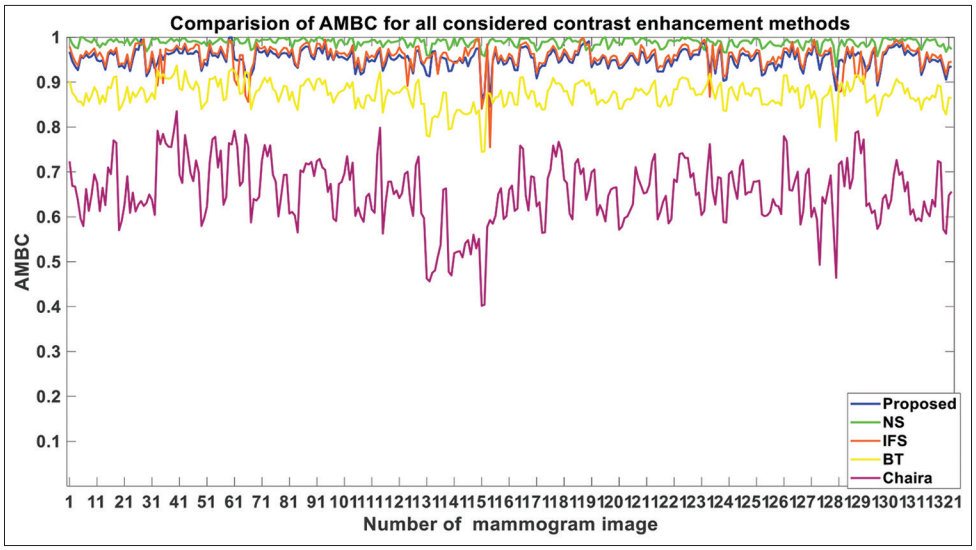

Figure 6: Comparative analysis of absolute mean brightness coefficient values for the applied enhancement methods. AMBC – absolute mean brightness coefficient

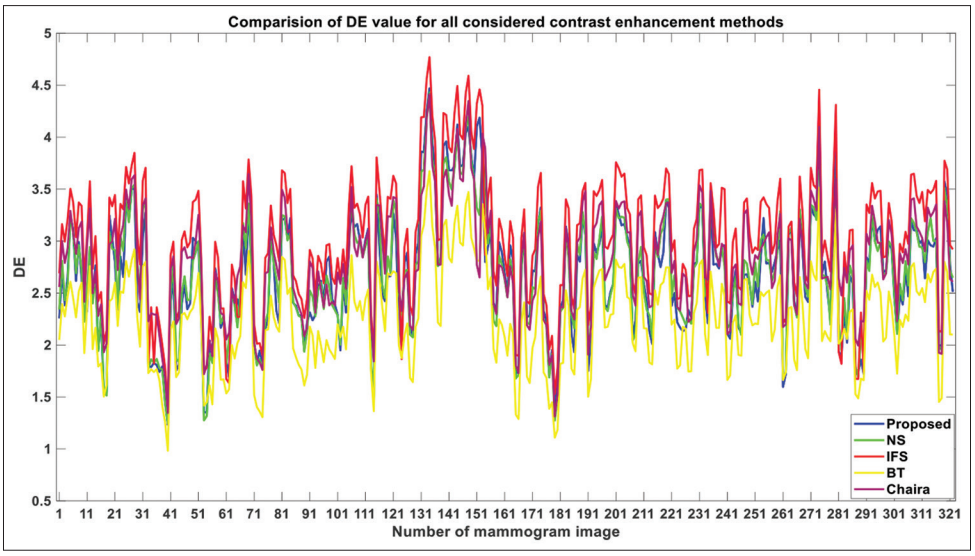

Figure 7: Comparative analysis of discrete entropy values for the applied enhancement methods. DE – Discrete entropy

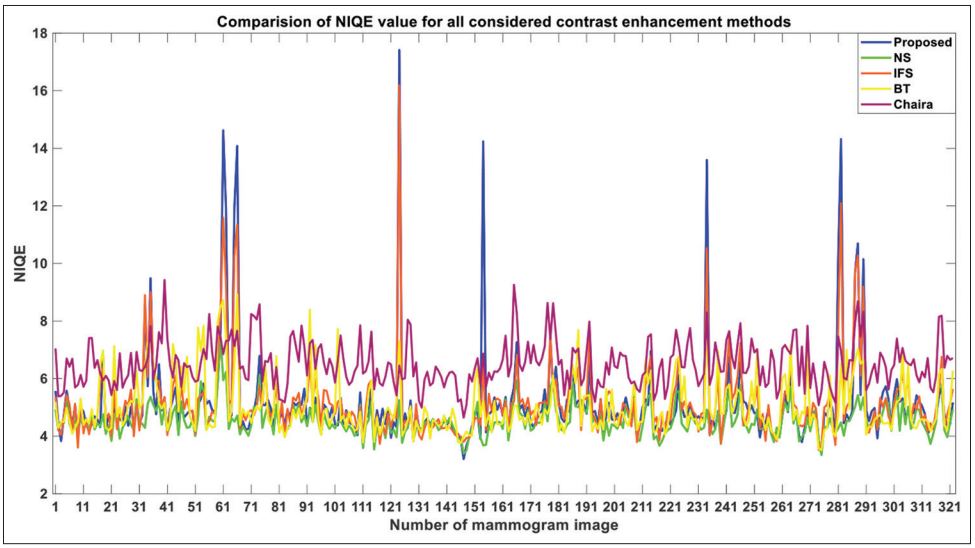

Figure 8: Comparative analysis of NIQE values for the applied enhancement methods

the NS method with an average of 4.5501 has the best performance in preserving the naturalness of the images. In this criterion, the proposed method, with an average of 5.1385, has a better performance compared to the IFS method, with an average of 5.1844. In this criterion, the BT method, with an average of 6.5129, shows the lowest performance in preserving the quality and naturalness of the images.

As previously noted, the enhancement of mammography image quality should be assessed from both qualitative and quantitative perspectives. A comparison of the quantitative results, specifically the average performance of evaluation metrics on images from the MIAS database presented in Table 1, alongside the sample images shown in Figure 2, indicates that the proposed method has achieved commendable outcomes relative to other methods, particularly when considering the qualitative results provided. Regarding the reasons for the superiority of the proposed method over others, in addition to the points highlighted in the analysis of experimental results, a key factor is the utilization of intuitive fuzzy entropy and NSs. These techniques effectively reduce ambiguity and enhance image contrast while preserving the quality and natural appearance of mammography images.

To investigate the significance of contrast improvement while maintaining image naturalness by the proposed method compared to other enhancement methods, the nonparametric Wilcoxon signed-rank statistical test was used, because all methods used a common database. The results of this test for the CII evaluation criterion, which is shown in Table 2, show that the contrast improvement

of the proposed method is statistically significant compared to all other methods with a *P* value of zero. This means that the proposed method has significantly improved the contrast of mammography images compared to other methods.

A rank-based Wilcoxon signed-rank test for the CII metric in Table 3 was performed comparing different methods against the proposed method. When comparing the NS method with the proposed method, 306 images of the MIAS dataset showed a negative rank (signifying less contrast enhancement than the proposed method) while 16 images showed a positive rank (signifying more contrast enhancement). When comparing the IFS method with the proposed method, 321 of 322 images had a negative rank and only 1 image had a positive rank, showing that the proposed method is significantly superior in increasing contrast of images compared to the IFS method. When comparing the BT method with the proposed method, all 322 images were negative. Similarly, when comparing the Chaira method with the proposed method, 321 images had a negative rank, and 1 image had a positive rank. These results confirm that the proposed method is significantly superior to other methods in increasing the contrast of mammogram images. These results highlight the significant advantage of the proposed method in obtaining increased contrast in the evaluated images compared to NS, IFS, BT, and Chaira methods.

In addition, the Wilcoxon signed-rank test was used to compare the NIQE metric between the proposed method and other improvement methods. The results presented in Table 4 show that the proposed method shows statistically significant improvement over NS, IF, and BT methods with a *P* value of 0. However, compared to the Chaira method, the proposed method produces a *P* value of 0.935, indicating that both methods have almost identical performance in preserving natural images.

The Wilcoxon signed-rank test performed to compare method rankings for the NIQE metric in Table 5 showed the following results:

When comparing the NS method with the proposed method, 265 images showed a negative rank, suggesting that the NS method outperforms the proposed method in maintaining the naturalistic nature of the image, as the lower NIQE value is associated with a more naturalistic image. Conversely, 57 images had a positive ranking, indicating that the proposed method for these images would have resulted in better performance. Overall, the NS method shows a higher performance for the NIQE metric. When comparing the IFS method and the proposed method, of the 322 images, 128 had a negative rank and 194 had a positive rank, suggesting that the proposed method is better than the IFS method at preserving the naturalness of the images. In comparison between the BT method and the proposed method, 17 images showed a negative rank while 305 showed a positive rank, which demonstrates that the proposed method is more effective in this context. In

Table 1: Average performance of enhancement methods

Methods	CII	AMBC	AMBE	DE	NIQE
Chaira[33]	0.8372	0.6543	0.1243	2.8073	5.0387
BT[34]	0.6991	0.8730	0.1467	2.2544	6.5129
IFS[11]	1.0455	0.9575	0.0453	3.0232	5.1844
NS[3]	1.2589	0.9885	0.0117	2.6821	4.5501
Proposed Method	1.4452	0.9517	0.0513	2.6718	5.1385

CII – Contrast improvement index; AMBC – Absolute mean brightness coefficient; AMBE – Absolute mean brightness error; NIQE – Naturalness image quality evaluator; DE – Discrete entropy; IFS – Intuitive fuzzy sets; NS – Neutrosophic set; BT – Bora-Thakur

Table 2: Results of the Wilcoxon signed-rank test for contrast improvement index

	Test statistics[a]			
	NS - proposed	IFS - proposed	BT - proposed	Chaira - proposed
Z	−13.022[b]	−15.549[b]	−15.552[b]	−15.552[b]
Asymptotic significant (two-tailed)	0.000	0.000	0.000	0.000

[a]Wilcoxon signed-rank test; [b]Based on positive ranks.
IFS – Intuitive fuzzy sets; NS – Neutrosophic set; BT – Bora-Thakur

Table 3: Results of the Wilcoxon rank test for contrast improvement index

	Ranks		
	n	Mean rank	Sum of ranks
NS - Proposed			
Negative ranks	306[a]	156.12	47,773.00
Positive ranks	16[b]	264.38	4230.00
Ties	0[c]		
Total	322		
IFS - Proposed			
Negative ranks	321[d]	161.98	51,997.00
Positive ranks	1[e]	6.00	6.00
Ties	0[f]		
Total	322		
BT - Proposed			
Negative ranks	322[g]	161.50	52,003.00
Positive ranks	0[h]	0.00	0.00
Ties	0[i]		
Total	322		
Chaira - Proposed			
Negative ranks	321[j]	162.00	52,002.00
Positive ranks	1[k]	1.00	1.00
Ties	0[l]		
Total	322		

[a]NS < Proposed; [b]NS > Proposed; [c]NS=Proposed; [d]IFS < Proposed; [e]IFS > Proposed; [f]IFS = Proposed; [g]BT < Proposed; [h]BT > Proposed; [i]BT=Proposed; [j]Chaira < Proposed; [k]Chaira > Proposed; [l]Chaira=Proposed. IFS – Intuitive fuzzy sets; NS – Neutrosophic set; BT – Bora-Thakur

Table 4: Results of the Wilcoxon signed-rank test for the natural image quality evaluator

Test statistics[a]				
	NS - Proposed	IFS - Proposed	BT - Proposed	Chaira – Proposed
Z	−12.721[b]	−3.722[c]	−13.221[c]	−0.081[c]
Asymptotic significant (two-tailed)	0.000	0.000	0.000	0.935

[a]Wilcoxon signed-ranks test; [b]Based on positive ranks; [c]Based on negative ranks. IFS – Intuitive fuzzy sets; NS – Neutrosophic set; BT – Bora-Thakur

Table 5: Results of the Wilcoxon rank test for natural image quality evaluator

Ranks			
	n	Mean rank	Sum of ranks
NS - Proposed			
Negative ranks	265[a]	178.38	47,270.00
Positive ranks	57[b]	83.04	4733.00
Ties	0[c]		
Total	322		
IFS - Proposed			
Negative ranks	128[d]	154.52	19,779.00
Positive ranks	194[e]	166.10	32,224.00
Ties	0[f]		
Total	322		
BT - Proposed			
Negative ranks	17[g]	229.29	3898.00
Positive ranks	305[h]	157.72	48,105.00
Ties	0[i]		
Total	322		
Chaira - Proposed			
Negative ranks	168[j]	153.96	25,866.00
Positive ranks	154[k]	169.72	26,137.00
Ties	0[l]		
Total	322		

[a]NS < Proposed; [b]NS > Proposed; [c]NS=Proposed; [d]IFS < Proposed; [e]IFS > Proposed; [f]IFS=Proposed; [g]BT < Proposed; [h]BT > Proposed; [i]BT=Proposed; [j]Chaira < Proposed; [k]Chaira > Proposed; [l]Chaira=Proposed. IFS – Intuitive fuzzy sets; NS – Neutrosophic set; BT – Bora-Thakur

comparison between the Chaira method and the proposed method, 168 images had a negative rank and 154 images a positive rank, indicating that the Chaira method and the proposed method have comparable performance in maintaining image naturalness.

These results highlight the different performance of the proposed method compared to NS, IFS, BT, and Chaira methods in terms of NIQE, with the proposed method showing a significant advantage over IFS and BT, but also showing a similar performance to Chaira.

In order to assess the quantitative performance of the proposed method and other enhancement methods used in this study using other databases, all experiments were carried out on 20 CBIS-DDSM images. Results obtained for the quantitative evaluation metrics discussed in Evaluation metrics are shown in Tables 6-9.

Table 6 shows the CII values for the different enhancement methods compared to the proposed method and the average performance of each of them. The proposed method achieves the highest mean CII of 1.1955, indicating the highest degree of contrast enhancement of any of the tested methods. In this comparison, the IFS method records an average CII value of 1.0114, while the BT method shows the lowest average CII value of 0.7852.

Table 7 shows the DE metric values for different enhancement methods compared to the proposed method and the average performance of each method. The proposed method achieves a lower entropy value of 2.6641 compared to the IFS method, which has an average DE of 2.8143, and the NS method, which has an average DE value of 2.6534. This lower entropy reflects the ability of the proposed method to reduce noise and improve detail in particular in the areas of the image that are mass-produced.

Table 8 compares AMBC and shows the performance of different enhancement methods in maintaining brightness. It can be noted that the proposed method provides optimal AMBC values for most images, which indicates that it is effective in preserving the naturalness of the original image.

Table 9 compares the AMBE values for various enhancement methods. The results show that the proposed method, with an average AMBE of 0.0248, achieves a relatively low AMBE value for the majority of images, demonstrating its effectiveness in enhancing contrast without significantly affecting brightness. In this comparison, the NS method exhibits the least impact on image brightness, with an average AMBE of 0.0090.

A comprehensive analysis of the quantitative results obtained from 20 images in the CBIS-DDSM dataset shows that the results are consistent with those in the MIAS dataset. Specifically, the proposed method achieves the highest CII value with an average of 1.1955, while the BT method records the lowest CII value with an average of 0.7852 among the evaluated methods. Table 7, which relates to DE, shows that the Chaira method has the highest level of uncertainty and randomness, with an average DE of 2.8742, compared with the other methods. Following the IFS method with an average DE of 2.8143, the proposed method has the next highest uncertainty and randomness at 2.6641. The NS method has an average DE of 2.6534. In this metric, BT has the lowest level of uncertainty and randomness compared to other methods, with an average of 2.0360. Table 8 of the AMBC metric shows that the NS method achieves the highest value, with an average of 0.9911, indicating that it is more efficient at preserving natural image brightness. The proposed method, with an average AMBC of 0.9761, is a commendable performance

Table 6: Evaluation of enhancement methods using contrast improvement index

Image	Chaira[33]	BT[34]	IFS[11]	NS[3]	Proposed method
Calc_Test_P_00038_RIGHT_CC	0.9197	0.7809	0.9889	0.8177	1.1939
Calc_Test_P_00041_LEFT_CC	0.8980	0.7907	0.9921	0.9236	1.1515
Calc_Test_P_00164_RIGHT_CC	0.8402	0.7742	1.0662	0.8509	1.2615
Calc_Test_P_00202_RIGHT_CC	0.8584	0.7618	1.0104	0.9979	1.1854
Calc_Test_P_00353_LEFT_CC	0.8968	0.7824	1.0146	1.1830	1.2228
Calc_Test_P_00372_RIGHT_CC	0.8975	0.7976	1.0253	1.1726	1.2424
Calc_Train_P_00049_RIGHT_CC	0.9735	0.9375	1.0066	1.1487	1.1658
Calc_Train_P_00016_LEFT_CC	0.8817	0.7863	1.0214	1.1364	1.1908
Calc_Train_P_00048_RIGHT_CC	0.8855	0.7778	1.0089	0.8130	1.1964
Calc_Train_P_00029_LEFT_CC	0.8717	0.7752	0.9910	0.9738	1.1581
Mass_Test_P_00194_RIGHT_CC	0.8597	0.7415	1.0116	1.1707	1.2059
Mass_Test_P_00016_LEFT_CC	0.8817	0.7863	1.0213	1.1364	1.1908
Mass_Test_P_00192_RIGHT_CC	0.9271	0.8005	0.9910	1.2212	1.2213
Mass_Test_P_00200_LEFT_CC	0.9454	0.8262	0.9846	0.5838	1.2003
Mass_Train_P_00116_RIGHT_CC	0.8366	0.7367	1.0929	1.0407	1.3369
Mass_Train_P_00001_LEFT_CC	0.8548	0.7573	1.0251	1.0921	1.2058
Mass_Train_P_00039_RIGHT_CC	0.8363	0.7544	1.0253	0.7874	1.2010
Mass_Train_P_00055_LEFT_CC	0.8701	0.7676	0.9887	1.1540	1.1224
Mass_Train_P_00076_RIGHT_CC	0.8968	0.7940	0.9911	0.9051	1.1376
Mass_Train_P_00058_LEFT_CC	0.9126	0.7749	0.9705	1.1306	1.1201
Average	0.8872	0.7852	1.0114	1.0120	1.1955

IFS – Intuitive fuzzy sets; NS – Neutrosophic set; BT – Bora-Thakur

Table 7: Evaluation of enhancement methods using discrete entropy

Image	Chaira[33]	BT[34]	IFS[11]	NS[3]	Proposed method
Calc_Test_P_00038_RIGHT_CC	2.2476	1.4321	2.1190	2.0084	1.9889
Calc_Test_P_00041_LEFT_CC	3.0236	2.0506	2.8988	2.8288	2.8149
Calc_Test_P_00164_RIGHT_CC	2.9596	2.3059	3.1795	2.9208	3.0077
Calc_Test_P_00202_RIGHT_CC	4.0705	3.0492	3.9590	3.7787	3.7772
Calc_Test_P_00353_LEFT_CC	3.2296	2.4400	3.1655	2.8585	2.8510
Calc_Test_P_00372_RIGHT_CC	2.1073	1.5034	2.0729	1.9110	1.9104
Calc_Train_P_00049_RIGHT_CC	2.1954	1.5685	2.2137	2.0329	2.0265
Calc_Train_P_00016_LEFT_CC	2.1751	1.5601	2.1363	2.0086	2.0101
Calc_Train_P_00048_RIGHT_CC	2.9722	2.1124	2.8532	2.7284	2.6950
Calc_Train_P_00029_LEFT_CC	3.2557	2.3672	3.1340	3.0390	3.0334
Mass_Test_P_00194_RIGHT_CC	2.8628	2.0335	2.7732	2.6241	2.6667
Mass_Test_P_00076_LEFT_CC	3.1146	2.2246	2.9843	2.8425	2.8406
Mass_Test_P_00192_RIGHT_CC	2.5533	1.7611	2.4280	2.2572	2.2572
Mass_Test_P_00200_LEFT_CC	2.6981	1.7378	2.5612	2.3098	2.3358
Mass_Test_P_00116_RIGHT_CC	1.9741	1.4580	2.1710	1.9700	2.0718
Mass_Train_P_00001_LEFT_CC	2.6969	1.6553	2.6610	2.5365	2.5301
Mass_Train_P_00039_RIGHT_CC	3.5982	2.7384	3.6190	3.4578	3.4393
Mass_Train_P_00055_LEFT_CC	2.6932	1.8373	2.6026	2.5277	2.5352
Mass_Train_P_00076_RIGHT_CC	3.1146	2.2246	2.9843	2.8425	2.8406
Mass_Train_P_00058_LEFT_CC	3.9412	2.6604	3.7697	3.5840	3.6495
Average	2.8742	2.0360	2.8143	2.6534	2.6641

IFS – Intuitive fuzzy sets; NS – Neutrosophic set; BT – Bora-Thakur

in the IFS method in maintaining natural brightness. On the other hand, the Chaira method has the lowest performance with an average AMBC of 0.6954, indicating that it is less efficient at preserving natural image brightness than other methods. Regarding the AMBE metric in Table 9, the NS method again shows the least impact on brightness during mammography contrast enhancement, with an average value of 0.0090. The proposed method, with an average AMBE of 0.0248, achieves a satisfactory performance in enhancing contrast without affecting brightness, following the IFS method. The BT method, with an average AMBE of 0.1240, has the highest value, indicating it is the least

Table 8: Evaluation of enhancement methods using absolute mean brightness coefficient

Image	Chaira[33]	BT[34]	IFS[11]	NS[3]	Proposed method
Calc_Test_P_00038_RIGHT_CC	0.8025	0.9324	0.9872	0.9975	0.9922
Calc_Test_P_00041_LEFT_CC	0.6786	0.8910	0.9880	0.9986	0.9894
Calc_Test_P_00164_RIGHT_CC	0.6122	0.8455	0.9368	0.9744	0.9270
Calc_Test_P_00202_RIGHT_CC	0.5791	0.8547	0.9814	0.9994	0.9813
Calc_Test_P_00353_LEFT_CC	0.6561	0.8718	0.9734	0.9870	0.9653
Calc_Test_P_00372_RIGHT_CC	0.7542	0.9046	0.9740	0.9882	0.9680
Calc_Train_P_00049_RIGHT_CC	0.7504	0.9041	0.9925	0.9861	0.9796
Calc_Train_P_00016_LEFT_CC	0.7370	0.9000	0.9820	0.9903	0.9751
Calc_Train_P_00048_RIGHT_CC	0.6716	0.8841	0.9872	0.9987	0.9842
Calc_Train_P_00029_LEFT_CC	0.6593	0.8784	0.9999	0.9906	0.9897
Mass_Test_P_00194_RIGHT_CC	0.7048	0.8941	0.9891	0.9917	0.9817
Mass_Test_P_00032_LEFT_CC	0.6933	0.8979	0.9962	0.9860	0.9879
Mass_Test_P_00192_RIGHT_CC	0.7616	0.9141	0.9999	0.9910	0.9910
Mass_Test_P_00200_LEFT_CC	0.8011	0.9322	0.9704	0.9936	0.9798
Mass_Train_P_00116_RIGHT_CC	0.7066	0.8847	0.9542	0.9872	0.9478
Mass_Train_P_00001_LEFT_CC	0.6924	0.8860	0.9771	0.9902	0.9704
Mass_Train_P_00039_RIGHT_CC	0.5774	0.8475	0.9626	0.9996	0.9625
Mass_Train_P_00055_LEFT_CC	0.7123	0.8910	0.9900	0.9944	0.9949
Mass_Train_P_00076_RIGHT_CC	0.6969	0.8918	0.9810	0.9886	0.9975
Mass_Train_P_00058_LEFT_CC	0.6606	0.8907	0.9505	0.9896	0.9564
Average	0.6954	0.8898	0.9787	0.9911	0.9761

IFS – Intuitive fuzzy sets; NS – Neutrosophic set; BT – Bora-Thakur

Table 9: Evaluation of enhancement methods using absolute mean brightness error

Image	Chaira[33]	BT[34]	IFS[11]	NS[3]	Proposed method
Calc_Test_P_00038_RIGHT_CC	0.0739	0.0726	0.0129	0.0025	0.0079
Calc_Test_P_00041_LEFT_CC	0.1425	0.1224	0.0122	0.0014	0.0111
Calc_Test_P_00164_RIGHT_CC	0.1200	0.1828	0.0675	0.0262	0.0787
Calc_Test_P_00202_RIGHT_CC	0.2051	0.1700	0.0189	0.0006	0.0190
Calc_Test_P_00353_LEFT_CC	0.1234	0.1470	0.0274	0.0132	0.0360
Calc_Test_P_00372_RIGHT_CC	0.0694	0.1054	0.0267	0.0119	0.0331
Calc_Train_P_00049_RIGHT_CC	0.0731	0.1061	0.0076	0.0141	0.0208
Calc_Train_P_00016_LEFT_CC	0.0816	0.1112	0.0184	0.0098	0.0255
Calc_Train_P_00048_RIGHT_CC	0.1345	0.1311	0.0129	0.0013	0.0160
Calc_Train_P_00029_LEFT_CC	0.1377	0.1384	0.0000	0.0094	0.0104
Mass_Test_P_00194_RIGHT_CC	0.1111	0.1184	0.0110	0.0083	0.0186
Mass_Test_P_00032_LEFT_CC	0.1253	0.1137	0.0038	0.0142	0.0122
Mass_Test_P_00192_RIGHT_CC	0.0825	0.0940	0.0000	0.0091	0.0090
Mass_Test_P_00200_LEFT_CC	0.0740	0.0728	0.0030	0.0065	0.0206
Mass_Train_P_00116_RIGHT_CC	0.0798	0.1304	0.0480	0.0130	0.0550
Mass_Train_P_00001_LEFT_CC	0.1078	0.1288	0.0234	0.0099	0.0305
Mass_Train_P_00039_RIGHT_CC	0.1875	0.1799	0.388	0.0004	0.0390
Mass_Train_P_00055_LEFT_CC	0.1151	0.1117	0.0101	0.0056	0.0051
Mass_Train_P_00076_RIGHT_CC	0.1157	0.1213	0.0101	0.0115	0.0025
Mass_Train_P_00058_LEFT_CC	0.1636	0.1227	0.0521	0.0104	0.0455
Average	0.1162	0.1240	0.0377	0.0090	0.0248

IFS – Intuitive fuzzy sets; NS – Neutrosophic set; BT – Bora-Thakur

effective in enhancing contrast without impacting brightness compared to other methods.

Therefore, the performance of the proposed method in enhancing image contrast remains consistent across both the CBIS-DDSM and MIAS dataset images.

Conclusion and Future Work

Radiologists face significant challenges in interpreting mammographic images due to their inherently low contrast, particularly in identifying masses in glandular and dense glandular breast tissues, where the color of masses

often resembles the white breast tissue. Additionally, distinguishing between benign and malignant masses – where benign masses typically exhibit uniform and regular boundaries, while malignant masses often have spiculated and irregular borders – poses further difficulties. Enhancing these images can significantly improve the accuracy of mass detection. This study introduced a hybrid method based on intuitionistic fuzzy sets and NSs for improving the quality of digital mammographic images. The proposed method was compared with various enhancement techniques, including those based on type-2 fuzzy sets, intuitionistic fuzzy sets, and NSs. Both qualitative and quantitative results, based on evaluation metrics, demonstrated that the proposed method effectively reduces ambiguity while preserving the natural appearance of images and enhancing the visibility of lesion details. The incorporation of the intuitionistic fuzzy entropy function within the defined intuitionistic set contributed to a reduction in image ambiguity. A key finding of this research is that defining an NS for the image derived from the previous stage, leveraging the indeterminate membership function of the NS to identify uncertain image information, led to substantial improvements in both quantitative and qualitative results compared to other methods.

Further research and investigation in this field remain necessary. As future work, one could explore the use of alternative functions in the indeterminate membership function of NSs to obtain uncertain image information, aiming to enhance both the qualitative and quantitative improvement of these images. In addition, the results obtained by different enhancement methods may be used for image segmentation for the purpose of improving the accuracy of mass detection and classification in computer-aided diagnostic systems.

Ethical approval

Ethical approval was not required for this study as it utilized only publicly available, anonymized datasets (MIAS and CBIS-DDSM).

Availability of data and materials

The MIAS and CBIS-DDSM Datasets used in this research can be publicly accessed through https://www.kaggle.com/datasets/kmader/mias-mammography and https://www.kaggle.com/datasets/awsaf49/cbis-ddsm-breast-cancer-image-dataset, respectively.

Financial support and sponsorship

No funding was received to assist with the preparation of this manuscript.

Conflicts of interest

The authors declare that they have no competing interests.

References

1. Simon S. Facts & Figures 2019: US Cancer Death Rate Has Dropped 27% in 25 Years. American Cancer Society; 2019.
2. Acharya UK, Faisal A, Singh M, Yadav R, Goswami U. Image Enhancement Using Tri-Histogram Equalization Technique. International Conference on Emerging Smart Computing and Informatics (ESCI). IEEE; 2024. p. 1-6.
3. Chaira T. A novel neutrosophic divergence score for enhancement of mammogram images. Soft Comput 2024;28:7409-16.
4. Dabass J, Dabass M, Dabass B. Enhancement of digital mammograms using intuitionistic fuzzy entropy function. J Image Proc Pattern Recogn Progress 2023;10:10-26.
5. Tripathy S, Swarnkar T. Unified preprocessing and enhancement technique for mammogram images. Procedia Comput Sci 2020;167:285-92.
6. Jenifer S, Parasuraman S, Kadirvelu A. Contrast enhancement and brightness preserving of digital mammograms using fuzzy clipped contrast-limited adaptive histogram equalization algorithm. Appl Soft Comput 2016;42:167-77.
7. Bhateja V, Misra M, Urooj S. Non-Linear Filters for Mammogram Enhancement. Singapore: Springer; 2020.
8. Chaira T, Ray AK. Fuzzy Image Processing and Applications with MATLAB. Boca Raton: CRC Press, 2017.
9. Chaira T. An intuitionistic fuzzy clustering approach for detection of abnormal regions in mammogram images. J Digit Imaging 2021;34:428-39.
10. Cherif S, Baklouti N, Hagras H, Alimi AM. Novel intuitionistic-based interval type-2 fuzzy similarity measures with application to clustering. IEEE Trans Fuzzy Syst 2022;30:1260-71.
11. Dabass J, Arora S, Vig R, Hanmandlu M. Mammogram Image Enhancement Using Entropy and CLAHE Based Intuitionistic Fuzzy Method. In: 2019 6th International Conference on Signal Processing and Integrated Networks (SPIN). IEEE; 2019. p. 24-9.
12. Dahiya S, Gosain A. A novel type-II intuitionistic fuzzy clustering algorithm for mammograms segmentation. J Ambient Intell Humanized Comput 2023;14:3793-808.
13. Montes I, Pal NR, Montes S. Entropy measures for Atanassov intuitionistic fuzzy sets based on divergence. Soft Comput 2018;22:5051-71.
14. Chaira T. Enhancement of medical images in an Atanassov's't intuitionistic fuzzy domain using an alternative intuitionistic fuzzy generator with application to image segmentation. J Intell Fuzzy Syst 2014;27:1347-59.
15. ChairaT. Intuitionistic fuzzy approach for enhancement of low contrast mammogram images. Int J Imaging Syst Technol 2020;30:1162-72.
16. Deng H, Deng W, Sun X, Liu M, Ye C, Zhou X. Mammogram enhancement using intuitionistic fuzzy sets. IEEE Trans Biomed Eng 2016;64:1803-14.
17. Chaira T. Contrast Enhancement of Medical Images Using Type II Fuzzy Set, of IEEE National Conference on Communications (NCC); 2013. p. 1-5.
18. Guo Y, Cheng H, Zhang Y. A new neutrosophic approach to image denoising. New Math Natl Comput 2009;5:653-62.
19. Bharti P, Mittal D. An ultrasound image enhancement method using neutrosophic similarity score. Ultrasonic Imaging 2020;42:271-83.
20. Shahin AI, Amin KM, Sharawi AA, Guo Y. A novel enhancement technique for pathological microscopic image using neutrosophic similarity score scaling. Optik 2018;161:84-97.
21. Guo Y, Şengür A, Ye J. A novel image thresholding algorithm based on neutrosophic similarity score. Measurement 2014;58:175-86.
22. Zadeh LA. Fuzzy sets, information and control. Inform Control 1965;8:338-53.

23. Atanassov KT. Intuitionistic Fuzzy Sets. Heidelberg: Springer; 1999.
24. De Luca A, Termini S. A definition of a nonprobabilistic entropy in the setting of fuzzy sets theory. In: Readings in Fuzzy Sets for Intelligent Systems. Naples- Italy: Elsevier; 1993. p. 197-202.
25. Lin J. Divergence measures based on the Shannon entropy. IEEE Trans Inform Theory 1991;37:145-51.
26. Chaira T, Ray AK. Segmentation using fuzzy divergence. Pattern Recogn Lett 2003;24:1837-44.
27. Tizhoosh HR, Fochem M. Fuzzy histogram hyperbolization for image enhancement. Proc EUFIT 1995;95:3.
28. Vlachos IK, Sergiadis GD. The role of entropy in intuitionistic fuzzy contrast enhancement. In: International Fuzzy Systems Association World Congress. Berlin, Hiedelberg: Springer; 2007. p. 104-13.
29. Vlachos IK, Sergiadis GD. Hesitancy Histogram Equalization. In: IEEE International Fuzzy Systems Conference; 2007. p. 1-6.
30. Chaira T. Neutrosophic set based clustering approach for segmenting abnormal regions in mammogram images. Soft Comput 2022;26:10423-33.
31. Suckling J. The Mammographic Images Analysis Society Digital Mammogram Database. In: Exerpta Medica. International Congress Series; 1994. p. 375-8.
32. Lee RS, Gimenez F, Hoogi A, Miyake KK, Gorovoy M, Rubin DL. A curated mammography data set for use in computer-aided detection and diagnosis research. Sci Data 2017;4:170177.
33. Chaira T. An improved medical image enhancement scheme using type II fuzzy set. Appl Soft Comput 2014;25:293-308.
34. Bora DJ, Thakur RS. An Efficient Technique for Medical Image Enhancement Based on Interval Type-2 Fuzzy Set Logic. Progress in Computing, Analytics and Networking: Proceedings of ICCAN; 2017. p. 667-78.